Articles

Magnetic Interactions in the High-Spin Iron(III) Oxooctaethylchlorinato Derivative [Fe(oxoOEC)(Cl)] and Its π-Cation Radical [Fe(oxoOEC$^{\bullet}$)(Cl)]$SbCl_6$

Teresa J. Neal,[†] Seong-Joo Kang,[†,‡] Ilona Turowska-Tyrk,[†,§] Charles E. Schulz,*[,||] and W. Robert Scheidt*[,†]

Department of Chemistry and Biochemistry, The University of Notre Dame, Notre Dame, Indiana 46556, and Department of Physics, Knox College, Galesburg, Illinois 61401

Received August 31, 1999

The preparation and characterization of the β-oxochlorin derivative [3,3,7,8,12,13,17,18-octaethyl-(3*H*)-porphin-2-onato(2−)]iron(III) chloride, [Fe(oxoOEC)(Cl)], and its π-cation radical derivative [Fe(oxoOEC$^{\bullet}$)(Cl)]$SbCl_6$ is described. Both compounds have been characterized by single-crystal X-ray structure determinations, IR, UV/vis/near-IR, and Mössbauer spectroscopies, and temperature-dependent magnetic susceptibility measurements. The macrocycles of [Fe(oxoOEC)(Cl)] and [Fe(oxoOEC$^{\bullet}$)(Cl)]$SbCl_6$ are both saddled, and [Fe(oxoOEC$^{\bullet}$)(Cl)]-$SbCl_6$ is slightly ruffled as well. [Fe(oxoOEC)(Cl)] shows a laterally shifted dimeric unit in the solid state, with a mean plane separation of 3.39 Å and a lateral shift of 7.39 Å. Crystal data for [Fe(oxoOEC)(Cl)]: triclinic, space group $P\bar{1}$, $Z = 2$, $a = 9.174(2)$ Å, $b = 13.522(3)$ Å, $c = 14.838(3)$ Å, $\alpha = 95.79(3)°$, $\beta = 101.46(2)°$, $\gamma = 104.84(3)°$. Upon oxidation, the inter-ring geometric parameters increase; the mean plane separation and the lateral shift of the dimeric unit of [Fe(oxoOEC$^{\bullet}$)(Cl)]$SbCl_6$ are 4.82 and 8.79 Å, respectively. Crystal data for [Fe(oxoOEC$^{\bullet}$)(Cl)]$SbCl_6$: monoclinic, space group Cc, $Z = 4$, $a = 19.8419(13)$ Å, $b = 10.027(2)$ Å, $c = 22.417-(4)$ Å, $\beta = 96.13(2)°$. A broad near-IR absorption band appears at 1415 nm for the π-cation radical, [Fe(oxoOEC$^{\bullet}$)-(Cl)]$SbCl_6$. Zero-field Mössbauer measurements at 4.2 K for both [Fe(oxoOEC)(Cl)] and [Fe(oxoOEC$^{\bullet}$)(Cl)]$SbCl_6$ confirmed that the oxidation state of the iron atom did not change upon chemical oxidation. Solid-state magnetic susceptibility measurements for [Fe(oxoOEC$^{\bullet}$)(Cl)]$SbCl_6$ resulted in a large temperature dependence of the magnetic moment that can best be fit with a model that includes a zero-field splitting parameter of $D = 6$ cm^{-1}, antiferromagnetic intermolecular iron−iron coupling ($2J_{Fe-Fe} = -0.14$ cm^{-1}), antiferromagnetic intramolecular iron−radical coupling ($2J_{Fe-r} = -76$ cm^{-1}), and antiferromagnetic radical−radical coupling ($2J_{r-r} = -13$ cm^{-1}).

Introduction

A number of heme proteins exhibit spin coupling between the iron atom and a nearby unpaired spin; for example, the oxidation of catalase and peroxidase by H_2O_2 is a two-electron process which leads to the formation of compound **I**, which contains an iron center that is weakly antiferromagnetically coupled to the porphyrin π-cation radical (intramolecular coupling).[1−5] However, detailed studies of magnetic interactions between iron metal centers and porphyrin π-cation radicals are extremely limited. Weiss and co-workers have investigated magnetic coupling in oxoferrylporphyrin (Fe(IV)═O) π-cation radical complexes[6−11] using Mössbauer and EPR spectroscopies; these *meso*-substituted species all showed ferromagnetic intramolecular coupling. Detailed modeling of intramolecular coupling appropriate for systems such as the catalases[12] and peroxidases[13−15] has been difficult since metalloporphyrin

* To whom correspondence should be addressed.
† The University of Notre Dame.
‡ Present address: Korean National University of Education, Chongwon, Korea.
§ Present address: Technical University of Wroclaw, Wroclaw, Poland.
|| Knox College.

(1) Schulz, C. E.; Rutter, R.; Sage, J. T.; Debrunner, P. G.; Hager, L. P. *Biochemistry* **1984**, *23*, 4743.
(2) Rutter, R.; Hager, L. P.; Dhonau, H.; Hendrich, M.; Valentine, M.; Debrunner, P. G. *Biochemistry* **1984**, *23*, 6809.
(3) Roberts, J. E.; Hoffman, B. M.; Rutter, R.; Hager, L. P. *J. Am. Chem. Soc.* **1981**, *103*, 7654.
(4) Roberts, J. E.; Hoffman, B. M.; Rutter, R.; Hager, L. P. *J. Biol. Chem.* **1981**, *256*, 2118.
(5) Schulz, C. E.; Devaney, P. W.; Winkler, H.; Debrunner, P. G.; Doan, N.; Chiang, R.; Rutter, R.; Hager, L. P. *FEBS Lett.* **1979**, *103*, 102.
(6) Gold, A.; Jayaraj, K.; Austin, R. N.; Ball, L. M.; Terner, J.; Mandon, D.; Weiss, R.; Fischer, J.; DeCian, A.; Bill, E.; Muther, M.; Schuneman, V.; Trautwein, A. X. *Inorg. Chem.* **1997**, *36*, 4555.
(7) Jayaraj, K.; Terner, J.; Gold, A.; Roberts, D. A.; Austin, R. N.; Mandon, D.; Weiss, R.; Bill, E.; Muther, M.; Trautwein, A. X. *Inorg. Chem.* **1996**, *35*, 1632.
(8) Jayaraj, K.; Gold, A.; Austin, R. N.; Mandon, D.; Weiss, R.; Terner, J.; Bill, E.; Muther, M.; Trautwein, A. X. *J. Am. Chem. Soc.* **1995**, *117*, 9079.
(9) Ochsenbein, P.; Mandon, D.; Fischer, J.; Weiss, R. *Angew. Chem.* **1993**, *32*, 1437.
(10) Mandon, D.; Weiss, R.; Jayaraj, K.; Gold, A.; Terner, J. *Inorg. Chem.* **1992**, *31*, 4404.
(11) Bill, E.; Ding, X.-Q.; Bominar, E. L.; Trautwein, A. X.; Winkler, H.; Mandon, D.; Weiss, R.; Gold, A.; Jayaraj, K.; Hatfield, W. E.; Kirk, M. L. *Eur. J. Biochem.* **1990**, *188*, 665.
(12) Corral, R. J. M.; Rodman, H. M.; Margolis, J.; Landau, B. R. *J. Biol. Chem.* **1974**, *249*, 3181.
(13) Augusto, O.; Schreiber, J.; Mason, R. P. *Biochem. Pharmacol.* **1988**, *37*, 2791.
(14) Meunier, B. *Biochimie* **1987**, *69*, 3.
(15) Ortiz de Montellano, P. R.; Grad, L. *Biochemistry* **1987**, *27*, 5310.

10.1021/ic991052w CCC: $19.00
Published on Web 02/10/2000

π-cation radical derivatives with alkyl substituents similar to naturally occurring systems are found to form dimeric systems.

In the π-cation radical systems studied to date, it has been found that relatively weak intermolecular (inter-ring) coupling of the π-cation radical electrons is observed in metallotetraphenylporphyrinate derivatives, [M(TPP$^{\bullet}$)],[16−19] while several four- and five-coordinate metallooctaethylporphyrinates, [M(OEP$^{\bullet}$)], show exceptionally strong intermolecular coupling of π-cation radical dimers.[20−22] The differences in the magnitude of the spin coupling are correlated with inter-ring structure, with relatively large inter-ring coupling constants being associated with the formation of tight cofacial $\pi-\pi$ dimers. For example, magnetic data for the iron tetraphenylporphyrinate π-cation radical, [Fe(TPP$^{\bullet}$)(Cl)]$SbCl_6$, revealed an overall $S = 2$ state (room-temperature moment 4.80 μ_B) implying that there was strong antiferromagnetic coupling of the $S = {}^5/_2$ iron atom and the $S = {}^1/_2$ porphyrin radical[23] (intramolecular coupling) and only very weak intermolecular coupling. In contrast, the crystal structure determination of the octaethylporphyrinate π-cation radical, [Fe(OEP$^{\bullet}$)(Cl)]ClO_4, revealed very tightly interacting cofacial dimers[22] with a lateral shift of 0.2 Å and a mean plane separation of 3.24 Å. The magnetic susceptibility data for this complex could be fit by two models, both of which gave a picture of strong coupling between the various spins in the dimeric species (large intermolecular coupling constants). The close $\pi-\pi$ interactions in several [M(OEP$^{\bullet}$)] dimers has been shown to result in strong antiferromagnetic coupling between the spins of the two radicals, even yielding diamagnetic pairs.[20]

The existence of [M(OEP$^{\bullet}$)] radical cations as tightly coupled diamagnetic pairs has precluded the detailed study of intramolecular interactions in these systems. Attempts at determining the intramolecular coupling component in π-cation radical systems containing a paramagnetic metal center have only been successful in systems containing peripheral substituents that are sterically demanding.[24−26] The introduction of bulky substituents at the periphery presumably prevents dimerization.

It is now known that porphyrin macrocycles containing a saturated ring display a wide range of functions in biological systems. More specifically, heme d_1, which consists of an unusual dioxoisobacteriochlorin,[28−33] is known to be involved in the function of bacterial nitrite reductases. Thus, metallo-β-oxochlorin derivatives can be viewed as model complexes for protein structures which contain heme d_1. We previously reported the magnetochemistry of [Cu(oxoOEC)] and the π-cation radical, [Cu(oxoOEC$^{\bullet}$)]$SbCl_6$,[27] whose macrocycles belong to the class of porphyrins that contain at least one saturated ring and a carbonyl group (β-oxoporphyrins). In this paper the preparation and complete characterization (structural, electronic, and magnetic) of two new iron(III) oxooctaethylchlorin (oxoOEC) complexes is presented. We use the *gem*-diethyl group of the oxochlorin ring to prevent the formation of tight cofacial $\pi-\pi$ dimers that is characteristic of all four- and five-coordinate metallooctaethylporphyrinate π-cation radicals. Exploitation of this special class of compounds has enabled us to assay both inter- and intramolecular coupling interactions in these π-cation radical systems.

Experimental Section

General Information. H_2OEP was synthesized by literature methods.[34] Iron(II) chloride was purchased from Acros, and tris(4-bromophenyl)aminium hexachloroantimonate was purchased from Aldrich. Dichloromethane and hexanes were distilled under argon from CaH_2 and sodium/benzophenone, respectively. Reactions involving the π-cation radical were performed under an argon atmosphere with oven-dried Schlenkware and cannula techniques.

Synthesis of [Fe(oxoOEC)(Cl)]. H_2(oxoOEC) was synthesized by modified literature procedures.[35−37] Insertion of iron metal into H_2(oxoOEC) was accomplished by the reaction of the free base and iron(II) chloride in DMF.[38] Crystals of [Fe(oxoOEC)(Cl)] were grown at room temperature by vapor diffusion of 3:2 CH_2Cl_2/hexanes into a 10 mg/mL CH_2Cl_2 solution of [Fe(oxoOEC)(Cl)]. UV/vis (CH_2Cl_2 solution): λ_{max} (log ϵ) 388 (Soret) (4.71), 549 (3.85), 601 (4.10) nm. IR (KBr): ν(CO) 1717 cm^{-1}.

Synthesis of [Fe(oxoOEC$^{\bullet}$)(Cl)]$SbCl_6$. [Fe(oxoOEC)(Cl)] (0.0207 g, 0.032 mmol) and tris(4-bromophenyl)aminium hexachloroantimonate (0.0270 g, 0.033 mmol) were placed in a 100-mL Schlenk flask and dried for 30 min under vacuum. After dichloromethane was added, the brown solution was stirred for 30 min. Black X-ray-quality crystals were obtained by transferring the solution to two 50-mL Schlenk flasks and layering with hexanes. UV/vis/near-IR (CH_2Cl_2): λ_{max} (log ϵ) 367 (Soret) (4.67), 507 (4.04), 589 (3.71), 1415 (3.20) nm. IR (KBr): ν(CO) 1737 cm^{-1}.

X-ray Structure Determinations. A dark purple crystal of [Fe(oxoOEC)(Cl)] and a black crystal of [Fe(oxoOEC$^{\bullet}$)(Cl)]$SbCl_6$ were examined on a Nonius FAST area-detector diffractometer at 127 K with a Mo rotating anode source ($\lambda = 0.710\ 73$ Å). Detailed methods and procedures for small-molecule X-ray data collection with the FAST system have been described elsewhere.[39] Intensity data were corrected for Lorentz and polarization effects.

The structure of [Fe(oxoOEC)(Cl)] was solved by the Patterson method, and the structure of [Fe(oxoOEC$^{\bullet}$)(Cl)]$SbCl_6$ was solved by

(16) Song, H.; Rath, N. P.; Reed, C. A.; Scheidt, W. R. *Inorg. Chem.* **1989**, *28*, 1839.
(17) Erler, B. S.; Scholz, W. F.; Lee, Y. J.; Scheidt, W. R.; Reed, C. A. *J. Am. Chem. Soc.* **1987**, *109*, 2644.
(18) Barkigia, K. M.; Spaulding, L. D.; Fajer, J. *Inorg. Chem.* **1983**, *22*, 349.
(19) Abbreviations used in this paper: OEP, octaethylporphyrin; (OEP$^{\bullet}$), the π-cation radical of OEP; TPP, tetraphenylporphyrin; OETPP, octaethyltetraphenylporphyrin; TMTMP, 2,7,12,17-tetramethyl-3,8,-13, 18-tetramesitylporphyrin; OEC, octaethylchlorin; oxoOEC (oxooctaethylchlorin), 3,3,7,8,12,13,17,18-octaethyl-(3*H*)-porphin-2-onato(2−); (oxoOEC$^{\bullet}$), the π-cation radical of oxoOEC.; dioxoOEiBC (dioxooctaethylisobacteriochlorin), 3,3,8,8,12,13,17,18-octaethyl-(3*H*,8*H*)-porphine-2,7-dionato; trioxoOEHP (trioxooctaethylhexahydroporphyrin), 3,3,7,8,12,12,18,18-octaethyl-(3*H*,12*H*,18*H*)-porphine-2,13,17-trionato; SQUID, superconducting quantum interference device.
(20) Song, H.; Orosz, R. D.; Reed, C. A.; Scheidt, W. R. *Inorg. Chem.* **1990**, *29*, 4274.
(21) Barkigia, K. M.; Renner, M. W.; Fajer, J. *J. Phys. Chem. B* **1997**, *101*, 8398.
(22) Schulz, C. E.; Song, H.; Mislanker, A.; Orosz, R. D.; Reed, C. A.; Debrunner, P. G.; Scheidt, W. R. *Inorg. Chem.* **1997**, *36*, 406.
(23) Gans, P.; Buisson, G.; Duee, E.; Marchon, J.-C.; Erler, B. S.; Scholz, W. F.; Reed, C. A. *J. Am. Chem. Soc.* **1986**, *108*, 1223.
(24) Renner, M. W.; Barkigia, K. M.; Zhang, Y.; Medforth, C. J.; Smith, K. M.; Fajer, J. *J. Am. Chem. Soc.* **1994**, *116*, 8562.
(25) Renner, M. W.; Barkigia, K. M.; Fajer, J. *Inorg. Chim. Acta* **1997**, *263*, 181.
(26) Fujii, H. *Inorg. Chem.* **1993**, *32*, 875.
(27) Neal, T. J.; Kang, S.-J.; Schulz, C. E.; Scheidt, W. R. *Inorg. Chem.* **1999**, *38*, 4294.
(28) Chang, C. K.; Timkovich, R.; Wu, W. *Biochemistry* **1986**, *25*, 8447.
(29) Wu, W.; Chang, C. K. *J. Am. Chem. Soc.* **1987**, *109*, 3149.
(30) Chang, C. K.; Wu, W. *J. Biol. Chem.* **1986**, *261*, 8593.
(31) Weeg-Aerssens, E.; Wu, W.; Ye, R. W.; Tiedje, J. M.; Chang, C. K. *J. Biol. Chem.* **1991**, *266*, 7496.
(32) Williams, P. A.; Fulop, V.; Garman, E. F.; Saunders: N. F. W.; Ferguson, S. J.; Hajdu, J. *Nature* **1997**, *389*, 406.
(33) Barkigia, K. M.; Chang, C. K.; Fajer, J.; Renner, M. W. *J. Am. Chem. Soc.* **1992**, *114*, 1701.
(34) Sessler, J.; Mozaffari, A.; Johnson, M. R. *Org. Synth.* **1992**, *70*, 68.
(35) Inhoffen, H. H.; Nolte, W. *Liebigs Ann. Chem.* **1969**, *725*, 167.
(36) Chang, C. K. *Biochemistry* **1980**, *19*, 1971.
(37) Chang, C. K.; Sotiriou, C. *J. Org. Chem.* **1985**, *50*, 4989.
(38) Adler, A. D.; Longo, F. R.; Kampas, F.; Kim. J. *J. Inorg. Nucl. Chem.* **1970**, *32*, 2443.
(39) Scheidt, W. R.; Turowska-Tyrk, I. *Inorg. Chem.* **1994**, *33*, 1314.

Table 1. Crystallographic Details for [Fe(oxoOEC)(Cl)] and [Fe(oxoOEC•(Cl)]$SbCl_6$

molecule	[Fe(oxoOEC)(Cl)]	[Fe(oxoOEC•(Cl)]$SbCl_6$
chem formula	$FeClN_4C_{36}OH_{44}\cdot 0.782CH_2Cl_2$	$FeCl_7N_4C_{36}OH_{44}Sb\cdot CH_2Cl_2$
fw	707.15	1059.43
a, Å	9.174(2)	19.8419(13)
b, Å	13.522(3)	10.027(2)
c, Å	14.838(3)	22.417(4)
α, deg	95.79(3)	90.00
β, deg	92.03(3)	96.13(2)
γ, deg	104.84(3)	90.00
V, Å^3	1766.6(6)	4434.6(12)
Z	2	4
space group	$P\bar{1}$	*Cc*
temp, K	130(2)	127(2)
D_c, g/cm^3	1.329	1.587
μ, mm^{-1}	0.656	1.513
final *R* indices [$I > 2\sigma(I)$]	$R_1 = 0.0950$, $wR_2 = 0.1687$	$R_1 = 0.0411$, $wR_2 = 0.1104$
final *R* indices (all data)	$R_1 = 0.1657$, $wR_2 = 0.2163$	$R_1 = 0.0583$, $wR_2 = 0.2061$

direct methods with the SHELXS-86 program.[40] Both structures were refined against F^2 with the SHELXL program. An absorption correction was applied at the final stages of the structure determination of [Fe(oxoOEC•)(Cl)]$SbCl_6$. All hydrogen atoms were idealized with the standard SHELXL idealization methods and were included in subsequent least-squares refinement cycles. The solvent region of the neutral species is described as a partially occupied methylene chloride molecule. Partial occupancy of the solvent molecule is not a requirement of crystallographic symmetry. Refinement of the methylene chloride molecule involved constraining the three atoms to the same final occupancy value. Brief crystallographic details for both structures are given in Table 1. Tables 2 and 3 list selected bond distances and angles for both complexes. Final atomic coordinates for both structures are included in the Supporting Information.

Physical Characterization. UV/vis/near-IR spectra were recorded on a Perkin-Elmer Lambda 19 UV/vis/near-IR spectrometer. IR spectra were recorded on a Perkin-Elmer 883 spectrometer. Mössbauer velocity scales are referred to the centroid of the room-temperature spectrum of a metallic iron foil. Samples of [Fe(oxoOEC•)(Cl)]$SbCl_6$ for Mössbauer spectroscopy were prepared by immobilization of ground crystals in Apiezon grease in the drybox. Magnetic susceptibility measurements were obtained on ground samples in the solid state over the temperature range 6−300 K on a Quantum Design MPMS SQUID susceptometer. Measurements at two fields (2 and 20 kG) showed that no ferromagnetic impurities were present; duplicate measurements ensured reproducibility among different sample preparations. χ_{diaM} was corrected for the underlying porphyrin ligand diamagnetism according to previous experimentally observed values;[41] all remaining diamagnetic contributions (χ_{dia}) were calculated using Pascal's constants.[42,43] All measurements included a correction for the diamagnetic sample holder and the diamagnetic immobilizing agent.

Results

The oxidation of [Fe(oxoOEC)(Cl)] with tris(4-bromophenyl)-aminium hexachloroantimonate results in the formation of the *π*-cation radical, [Fe(oxoOEC•)(Cl)]$SbCl_6$. The electronic spectrum of the oxidized complex (Figure 1) has a blue-shifted and broadened Soret band, the bands in the visible region have decreased in intensity, and a very broad near-IR band appears at 1415 nm. In the infrared, the carbonyl band at 1717 cm^{-1} for the neutral compound, [Fe(oxoOEC)(Cl)], shifts to 1737 cm^{-1} upon formation of the *π*-cation radical, [Fe(oxoOEC•)(Cl)]$SbCl_6$. In the oxidized species, a new IR band similar to the radical marker band in OEP *π*-cation radical derivatives[44,45] is seen at 1546 cm^{-1}.

The molecular structures of [Fe(oxoOEC)(Cl)] and the one-electron oxidation product, [Fe(oxoOEC•)(Cl)]$SbCl_6$, have been determined by X-ray crystallography. Figures 2 and 3 show a

Table 2. Summary of Bond Lengths for [Fe(oxoOEC)(Cl)] and the *π*-Cation Radical [Fe(oxoOEC•(Cl)]$SbCl_6$

	bond lengths (Å)	
	[Fe(oxoOEC)(Cl)]	[Fe(oxoOEC•(Cl)]$SbCl_6$
Fe(1)−N(1)	2.058(4)	2.060(5)
Fe(1)−N(2)	2.059(5)	2.049(5)
Fe(1)−N(3)	2.066(4)	2.046(6)
Fe(1)−N(4)	2.125(5)	2.106(6)
Fe(1)−Cl(1)	2.217(2)	2.196(2)
N(1)−C(a1)	1.378(7)	1.361(9)
N(1)−C(a2)	1.386(6)	1.390(8)
N(2)−C(a3)	1.367(7)	1.362(8)
N(2)−C(a4)	1.381(6)	1.367(8)
N(3)−C(a5)	1.386(7)	1.395(9)
N(3)−C(a6)	1.371(7)	1.366(8)
N(4)−C(a7)	1.367(7)	1.382(8)
N(4)−C(a8)	1.350(7)	1.376(9)
C(a1)−C(b1)	1.438(7)	1.462(9)
C(a2)−C(b2)	1.452(7)	1.443(10)
C(a3)−C(b3)	1.429(7)	1.467(9)
C(a4)−C(b4)	1.432(7)	1.456(9)
C(a5)−C(b5)	1.435(7)	1.464(9)
C(a6)−C(b6)	1.452(7)	1.455(10)
C(a7)−C(b7)	1.479(8)	1.487(10)
C(a8)−C(b8)	1.514(8)	1.474(9)
C(b1)−C(b2)	1.353(8)	1.327(11)
C(b3)−C(b4)	1.378(7)	1.357(9)
C(b5)−C(b6)	1.359(8)	1.354(11)
C(b7)−C(b8)	1.507(8)	1.512(10)
C(a2)−C(m1)	1.382(7)	1.389(10)
C(a3)−C(m1)	1.398(7)	1.375(10)
C(a4)−C(m2)	1.394(7)	1.386(9)
C(a5)−C(m2)	1.379(8)	1.391(9)
C(a6)−C(m3)	1.393(8)	1.363(10)
C(a7)−C(m3)	1.367(8)	1.374(10)
C(a8)−C(m4)	1.380(8)	1.366(9)
C(a1)−C(m4)	1.402(8)	1.386(10)
C(b7)−O(2)	1.239(7)	
C(b8)−O(1)		1.220(9)

(40) Programs used in this study included SHELXS-86 (Sheldrick, G. M. *Acta Crystallogr., Sect. A* **1990**, *A46*, 467), SHELXL-93 (Sheldrick, G. M. *J. Appl. Crystallogr.*, manuscript in preparation), and local modifications of ORTEP (Johnson, C. K. *ORTEP: A Fortran Thermal-Ellipsoid Plot Program For Crystal Structure Illustrations*; **1970**, Oak Ridge National Laboratory: Oak Ridge, TN, 1970). Scattering factors were taken from: *International Tables for Crystallography*; Wilson, A. J. C., Ed.; Kluwer Academic Publishers: Dordrecht, The Netherlands, 1992; Vol. C.

(41) Sutter, T. P. G.; Hambright, P.; Thorpe, A. N.; Quoc, N. *Inorg. Chim. Acta* **1992**, *195*, 131.

(42) Earnshaw, A. *Introduction to Magnetochemistry*; Academic: London, 1968; Chapter 1.

(43) Selwood, P. W. *Magnetochemistry*; Interscience: New York, 1956; Chapter 2.

(44) Hu, S.; Spiro, T. G. *J. Am. Chem. Soc.* **1993**, *115*, 12029.

(45) Shimomura, E. T.; Phillippi, M. A.; Goff, H. M.; Scholz, W. F.; Reed, C. A. *J. Am. Chem. Soc.* **1981**, *103*, 6778.

Table 3. Summary of Bond Angles for [Fe(oxoOEC)(Cl)] and the π-Cation Radical [Fe(oxoOEC$^{\bullet}$(Cl)]$SbCl_6$

	bond angles (deg)	
	[Fe(oxoOEC)(Cl)]	[Fe(oxoOEC$^{\bullet}$(Cl)]$SbCl_6$
N(1)−Fe(1)−N(2)	87.5(2)	87.9(2)
N(2)−Fe(1)−N(3)	87.9(2)	88.1(2)
N(3)−Fe(1)−N(4)	87.2(2)	86.1(2)
N(1)−Fe(1)−N(4)	86.7(2)	86.4(2)
N(1)−Fe(1)−N(3)	152.0(2)	154.4(2)
N(2)−Fe(1)−N(4)	157.7(2)	153.7(2)
N(1)−Fe(1)−Cl(1)	102.94(13)	100.1(2)
N(2)−Fe(1)−Cl(1)	105.86(13)	103.8(2)
N(3)−Fe(1)−Cl(1)	104.85(13)	105.4(2)
N(4)−Fe(1)−Cl(1)	96.40(13)	102.5(2)
C(a1)−N(1)−Fe(1)	127.2(4)	127.5(4)
C(a2)−N(1)−Fe(1)	125.9(3)	124.5(5)
C(a1)−N(1)−C(a2)	105.3(4)	105.1(5)
C(a3)−N(2)−Fe(1)	126.7(3)	126.9(5)
C(a4)−N(2)−Fe(1)	126.3(4)	126.3(4)
C(a3)−N(2)−C(a4)	105.6(4)	105.8(5)
C(a5)−N(3)−Fe(1)	126.0(4)	125.7(5)
C(a6)−N(3)−Fe(1)	127.0(4)	126.9(5)
C(a6)−N(3)−C(a5)	105.4(4)	105.2(6)
C(a7)−N(4)−Fe(1)	122.4(4)	126.1(5)
C(a8)−N(4)−Fe(1)	125.1(4)	124.3(4)
C(a8)−N(4)−C(a7)	109.8(5)	108.6(6)
N(1)−C(a1)−C(b1)	110.4(5)	110.6(6)
N(1)−C(a2)−C(b2)	110.3(5)	109.8(6)
N(2)−C(a3)−C(b3)	111.1(5)	110.7(6)
N(2)−C(a4)−C(b4)	110.5(4)	110.9(5)
N(3)−C(a5)−C(b5)	110.5(5)	110.3(6)
N(3)−C(a6)−C(b6)	110.4(5)	111.0(7)
N(4)−C(a7)−C(b7)	109.8(5)	113.0(6)
N(4)−C(a8)−C(b8)	112.5(5)	109.7(6)
N(1)−C(a1)−C(m4)	124.4(5)	123.5(6)
N(1)−C(a2)−C(m1)	124.9(5)	124.8(6)
N(2)−C(a3)−C(m1)	123.7(5)	125.0(6)
N(2)−C(a4)−C(m2)	124.3(5)	125.3(6)
N(3)−C(a5)−C(m2)	125.0(5)	124.2(6)
N(3)−C(a6)−C(m3)	124.6(5)	125.2(7)
N(4)−C(a7)−C(m3)	127.5(5)	123.9(7)
N(4)−C(a8)−C(m4)	125.2(5)	127.0(6)
C(m4)−C(a1)−C(b1)	125.0(5)	125.9(7)
C(m1)−C(a2)−C(b2)	124.7(5)	125.4(6)
C(m1)−C(a3)−C(b3)	125.2(5)	124.2(6)
C(m2)−C(a4)−C(b4)	125.2(5)	123.8(6)
C(m2)−C(a5)−C(b5)	124.5(5)	125.4(6)
C(m3)−C(a6)−C(b6)	125.0(5)	123.8(6)
C(m3)−C(a7)−C(b7)	122.7(5)	122.8(6)
C(m4)−C(a8)−C(b8)	122.3(5)	123.3(6)
C(b2)−C(b1)−C(a1)	107.6(5)	106.4(6)
C(b1)−C(b2)−C(a2)	106.3(5)	107.8(6)
C(b4)−C(b3)−C(a3)	106.5(5)	106.1(6)
C(b3)−C(b4)−C(a4)	106.4(5)	106.4(6)
C(b6)−C(b5)−C(a5)	107.0(5)	106.1(6)
C(b5)−C(b6)−C(a6)	106.6(5)	107.3(6)
C(b8)−C(b7)−C(a7)	106.9(5)	101.1(6)
C(b7)−C(b8)−C(a8)	100.9(5)	107.2(6)
C(a2)−C(m1)−C(a3)	126.5(5)	126.2(6)
C(a5)−C(m2)−C(a4)	126.7(5)	126.0(6)
C(a7)−C(m3)−C(a6)	125.9(5)	126.8(6)
C(a8)−C(m4)−C(a1)	126.5(5)	126.1(7)
O(2)−C(b7)−C(a7)	126.3(6)	
O(2)−C(b7)−C(b8)	126.9(5)	
O(1)−C(b8)−C(b7)		127.5(6)
O(1)−C(b8)−C(a8)		125.2(6)

labeled ORTEP diagram and a formal diagram giving the perpendicular displacements of each atom from the 24-atom mean plane for [Fe(oxoOEC)(Cl)] and the π-cation radical, [Fe(oxoOEC$^{\bullet}$)(Cl)]$SbCl_6$, respectively.

Individual bond lengths and angles for the pyrrolinone[46] ring and averaged bond lengths for the pyrrole rings are also displayed in Figures 2b and 3b. The estimated standard uncertainties are shown in parentheses; the uncertainties of the bond parameters reported for the pyrrolinone ring are those of the individual bond lengths and angles, while the numbers in parentheses of the remaining bond parameters represent the esds calculated for the averaged bond lengths and angles of the pyrrole rings.

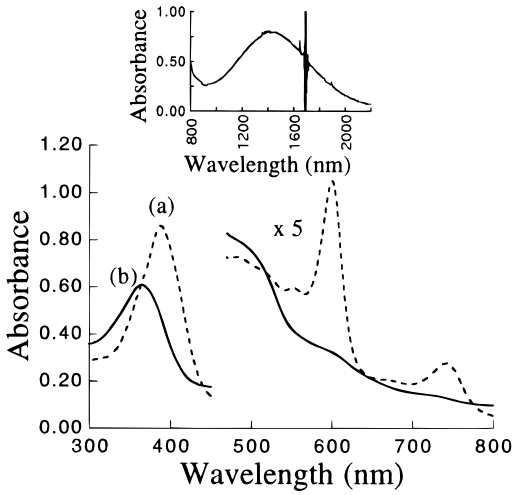

Figure 1. UV/visible spectra of (a) [Fe(oxoOEC)(Cl)] (1.66×10^{-4} M) and (b) the π-cation radical [Fe(oxoOEC)(Cl)]$SbCl_6$ (1.31×10^{-4} M) in CH_2Cl_2. The spectra on the left side of the plot were collected using a 1 mm cell; the spectra on the right were collected using a 10 mm cell. The upper inset shows the near-IR band of the π-cation radical [Fe(oxoOEC)(Cl)]$SbCl_6$ (5.0×10^{-4} M).

Edge-on and top-down views of the closest interacting "dimeric" pairs of [Fe(oxoOEC)(Cl)] are shown in Figure 4; the two rings are related by an inversion center. Figure 5 shows the corresponding views for [Fe(oxoOEC$^{\bullet}$)(Cl)]$SbCl_6$; the two rings are translation related. The intermolecular geometries (Fe···Fe distance, Ct···Ct distance, mean plane separation, and lateral shift) for each dimeric unit are summarized in Table 4.

Mössbauer spectra of [Fe(oxoOEC)(Cl)] and [Fe(oxoOEC$^{\bullet}$)(Cl)]$SbCl_6$ in a zero applied magnetic field display a single quadrupole doublet (Figure S1 in Supporting Information). The quadrupole doublets and isomer shifts at 4.2 K are ΔE_q 0.83 mm/s and δ_{Fe} 0.47 mm/s for neutral [Fe(oxoOEC)(Cl)], and ΔE_q 0.70 mm/s and δ_{Fe} 0.56 mm/s for the π-cation radical, [Fe(oxoOEC$^{\bullet}$)(Cl)]$SbCl_6$. The Mössbauer parameters for [Fe(oxoOEC)(Cl)] and [Fe(oxoOEC$^{\bullet}$)(Cl)]$SbCl_6$ are compared to those of other iron porphyrinate derivatives in Table 5.

Temperature-dependent (6−300 K) magnetic susceptibility measurements were carried out for [Fe(oxoOEC)(Cl)] and [Fe(oxoOEC$^{\bullet}$)(Cl)]$SbCl_6$. [Fe(oxoOEC)(Cl)] has a room-temperature magnetic moment of 5.90 μ_B and shows a temperature dependence typical of high-spin iron(III) porphyrinate complexes (Figure 6a). In contrast, [Fe(oxoOEC$^{\bullet}$)(Cl)]$SbCl_6$ has a magnetic moment with a large temperature dependence. Figure 6b shows the temperature dependence of the magnetic moment for [Fe(oxoOEC$^{\bullet}$)(Cl)]$SbCl_6$.

Discussion

Spectroscopic Properties. The oxidation of [Fe(oxoOEC)(Cl)] results in spectral changes consistent with the formation of a π-cation radical. In the UV, the Soret band blue-shifts and broadens upon oxidation; the bands in the visible region decrease in intensity and broaden upon oxidation (see Figure 1). In addition, a very broad near-IR band is observed at 1415 nm; the neutral (unoxidized) [Fe(oxoOEC)(Cl)] complex does not

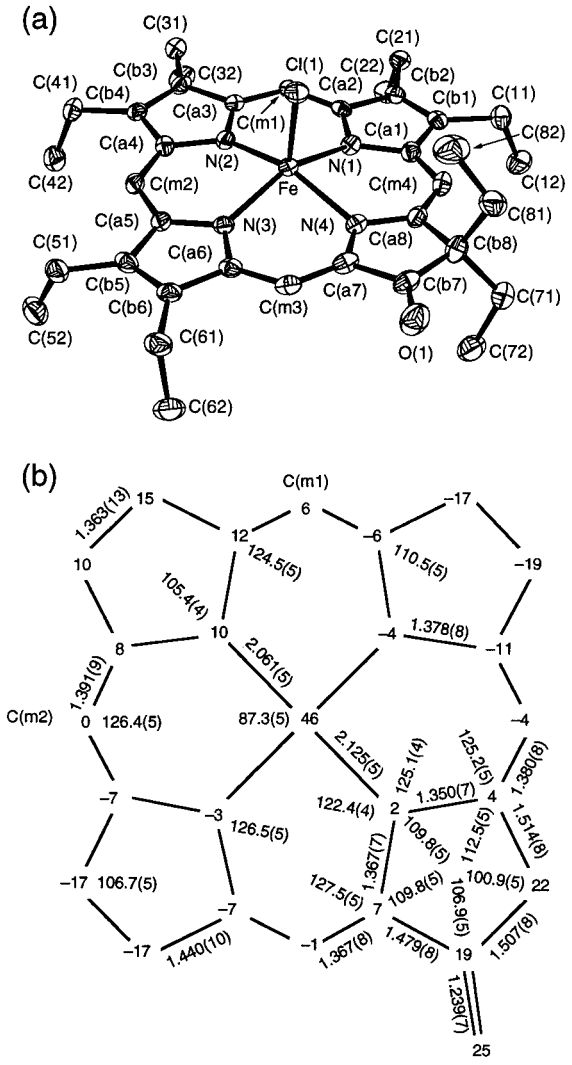

Figure 2. (a) Labeled ORTEP diagram of [Fe(oxoOEC)(Cl)]. Thermal ellipsoids are drawn to illustrate 50% probability surfaces. (b) Formal diagram giving the perpendicular displacements of each atom from the 24-atom mean plane of [Fe(oxoOEC)(Cl)] (in Å × 10^2). All bond lengths and angles of the pyrrolinone ring are shown. The remaining bond lengths and angles are averages of those for the pyrrole rings. The estimated standard uncertainties are shown in parentheses; the uncertainties of the bond parameters reported for the pyrrolinone ring are those of the individual bond lengths and angles, while the numbers in parentheses of the remaining bond parameters represent the esds calculated for the averaged bond lengths and angles of the pyrrole rings.

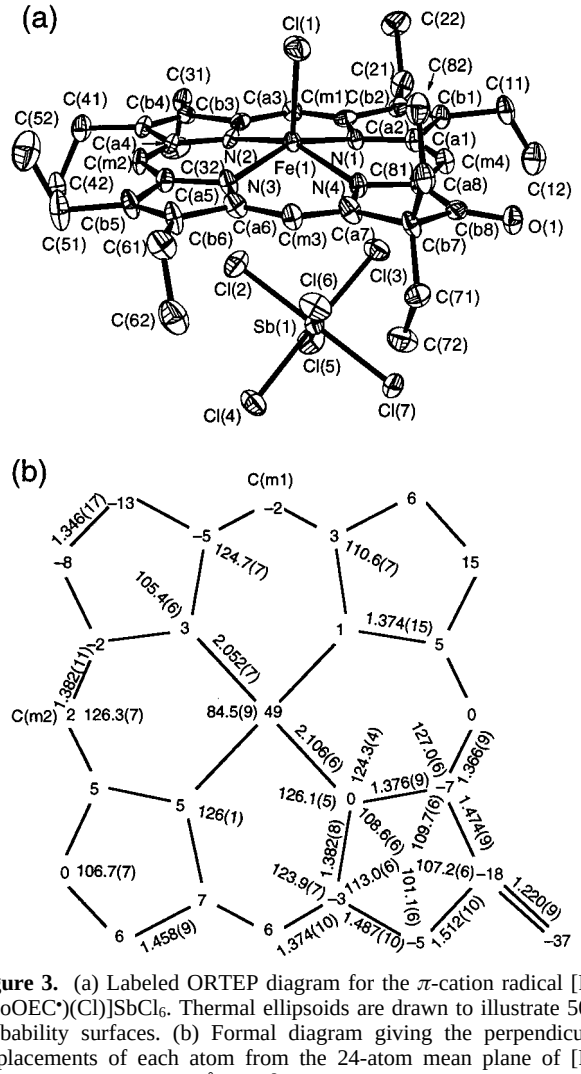

Figure 3. (a) Labeled ORTEP diagram for the π-cation radical [Fe(oxoOEC•)(Cl)]$SbCl_6$. Thermal ellipsoids are drawn to illustrate 50% probability surfaces. (b) Formal diagram giving the perpendicular displacements of each atom from the 24-atom mean plane of [Fe(oxoOEC•)(Cl)]$SbCl_6$ (in Å × 10^2). All bond lengths and angles of the pyrrolinone ring are shown. The remaining bond lengths and angles are averages of those for the pyrrole rings. The estimated standard uncertainties are shown in parentheses; the uncertainties of the bond parameters reported for the pyrrolinone ring are those of the individual bond lengths and angles, while the numbers in parentheses of the remaining bond parameters represent the esds calculated for the averaged bond lengths and angles of the pyrrole rings.

absorb in this region. This new, near-IR band, illustrated in the inset of Figure 1, requires some further elaboration.

Near-IR bands have been observed in metallooctaethylporphyrin π-cation radicals,[47−49] where they result from the formation of dimeric π-cation radical species, $[M(OEP^{\bullet})]_2^{2+}$. Broad absorption maxima are found at 900−960 nm for nickel, copper, palladium, and zinc octaethylporphyrin π-cation radicals. The π-cation radical complex of vanadyl octaethylporphyrin, $[VO(OEP^{\bullet})(H_2O)]SbCl_6$,[50] has a red-shifted near-IR band at 1375 nm. Similarly, the π-cation radical complex of the copper oxooctaethylchlorin, $[Cu(oxoOEC^{\bullet})]_2^{2+}$,[27] has two overlapped near-IR absorption bands at 1285 and 1548 nm that are significantly broader than those seen for the OEP species. All of these near-IR absorption bands are strongly concentration dependent. A plot of the absorbance against concentration for these systems reveals deviations from linearly at higher concentrations; the absorbance was larger at higher concentrations. The behavior of this band is consistent with that of a monomer−dimer equilibrium:

$$2[M(OEP^{\bullet})]^{+} \overset{K_D}{\rightleftharpoons} [M(OEP^{\bullet})]_2^{2+}$$

The magnitudes of the equilibrium constants for this reaction were found to range from ∼50 to 1100 M^{-1}.

(46) Other terms commonly used to describe the ring that contains a carbonyl group include "pyrrolidinone", "pyrrolidine", and "pyrroline".
(47) Brancato-Buentello, K. E.; Kang, S.-J.; Scheidt, W. R. *J. Am. Chem. Soc.* **1997**, *119*, 2839.
(48) Fuhrhop, J. H.; Wasser, P.; Riesner, D.; Mauzerall, D. *J. Am. Chem. Soc.* **1972**, *94*, 7996.
(49) Fajer, J.; Borg, D. C.; Forman, A.; Dolphin, D.; Felton, R. H. *J. Am. Chem. Soc.* **1970**, *92*, 3451.
(50) Schulz, C. E.; Song, H.; Lee, Y. J.; Mondal, J. U.; Mohanrao, K.; Reed, C. A.; Walker, F. A.; Scheidt, W. R. *J. Am. Chem. Soc.* **1994**, *116*, 7196.

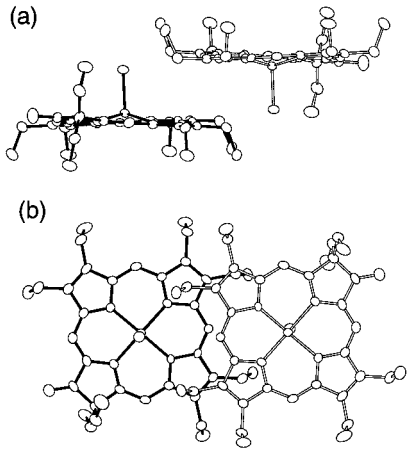

Figure 4. (a) Edge-on and (b) top-down views of the closest inversion-related dimeric unit of [Fe(oxoOEC)(Cl)].

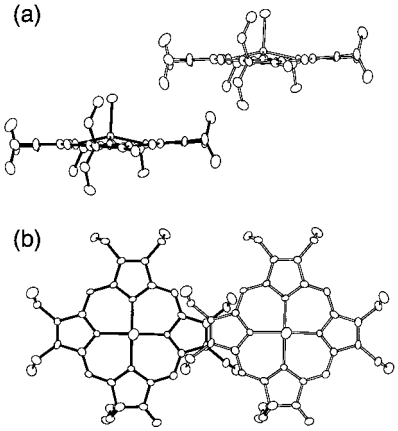

Figure 5. (a) Edge-on and (b) top-down views of the closest translation-related dimeric unit of the π-cation radical [Fe(oxoOEC$^{\bullet}$)-(Cl)]$SbCl_6$.

Table 4. Comparison of Geometry among Dimers of [Fe(oxoOEC)(Cl)] and the π-Cation Radical [Fe(oxoOEC$^{\bullet}$(Cl)]$SbCl_6$

compd	M···M	Ct···Ct[a]	MPS[b]	LS[c]
[Fe(oxoOEC)(Cl)]	7.77	8.13	3.39	7.39
[Fe(oxoOEC$^{\bullet}$(Cl)]$SbCl_6$	10.03	10.03	4.82	8.79

[a] Ct is the center of a 24-atom porphyrin ring. [b] The average mean plane separation for the two 24-atom cores of the dimer. [c] Lateral shift between the two 24-atom cores of the dimer.

Table 5. Mössbauer Parameters of [Fe(oxoOEC)(Cl)], [Fe(oxoOEC$^{\bullet}$(Cl)]$SbCl_6$, and Other Iron Porphyrinate Derivatives

compd	iron ox. state	iron spin state S	δ_{Fe}	ΔE_q	ref
[Fe(oxoOEC)(Cl)]	3	$^5/_2$	0.47	0.83	this work
[Fe(oxoOEC$^{\bullet}$(Cl)][$SbCl_6$]	3	$^5/_2$	0.56	0.70	this work
[Fe(OEP)(Cl)]	3	$^5/_2$	0.41	0.93	64
[Fe(TPP)(Cl)]	3	$^5/_2$	0.41	0.46	51
[Fe(TPP$^{\bullet}$(Cl)][$SbCl_6$]	3	$^5/_2$	0.40	0.55	62
[Fe(OEP$^{\bullet}$(Cl)][ClO_4]	3	$^5/_2$	0.42	0.71	22
[Fe(OEP$^{\bullet}$(Cl)][$SbCl_6$]	3	$^5/_2$	0.41	0.77	22
horseradish peroxidase compd I	4	1	0.00	1.20	63

A concentration-dependent spectral study for the π-cation radical [Fe(oxoOEC$^{\bullet}$)(Cl)]$SbCl_6$ was carried out over the concentration range 1.04×10^{-6} to 2.0×10^{-3} M. Surprisingly, the absorbance of the near-IR absorption band in [Fe(oxoOEC$^{\bullet}$)-(Cl)]$SbCl_6$ does not show any concentration-dependent behavior

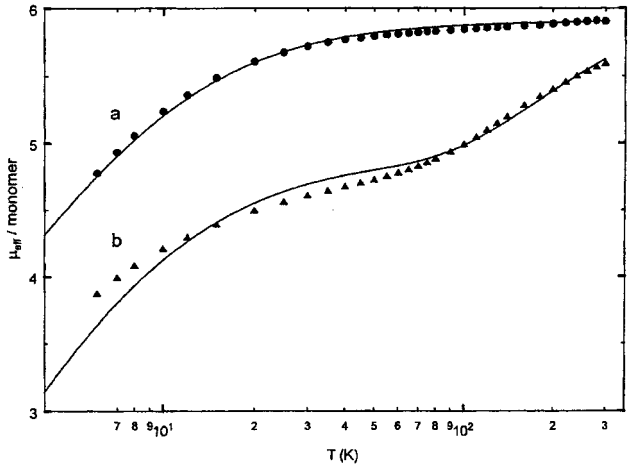

Figure 6. Comparison of observed and calculated values of μ_{eff}/monomer vs T for (a) [Fe(oxoOEC)(Cl)] and (b) [Fe(oxoOEC$^{\bullet}$)(Cl)]-$SbCl_6$. The solid lines are model calculations assuming pairwise spin coupling. The parameters used are (a) $S = {}^5/_2$ with axial zero-field splitting $D = 6$ cm^{-1} and an antiferromagnetic iron−iron interaction $2J_{Fe-Fe} = -0.28$ cm^{-1} and (b) $S = {}^5/_2$ and $s = {}^1/_2$ with axial zero-field splitting $D = 6$ cm^{-1}, $2J_{Fe-Fe} = -0.14$ cm^{-1}, $2J_{Fe-r} = -76$ cm^{-1}, and $2J_{r-r} = -13$ cm^{-1}.

(see Figure S2 in Supporting Information). Although thorough investigations involving the concentration-dependence of near-IR bands is limited,[47−49] the concentration-independent behavior of the near-IR band in this [Fe(oxoOEC$^{\bullet}$)(Cl)]$SbCl_6$ system is unique. The results indicate the presence of only one species (either a monomer or a dimer) over the investigated concentration range. If the dimeric species predominates (the solution is comprised of dimeric units even at 1.04×10^{-6} M), the equilibrium constant must be greater than 2×10^9 M^{-1}. If the monomeric species predominates (no dimerization occurs even at 2.0×10^{-3} M), the equilibrium constant must be less than $\sim$ 10 M^{-1}. This latter value, which presumes that the monomeric species predominates in solution over the concentration range that was studied, is more consistent with the results found for the dimeric octaethylporphyrin π-cation radical dimers mentioned above. Assuming that monomers predominate in solution, then the observed broad near-IR absorption band must be the result of an electronic transition which accompanies the formation of the oxidized (π-cation radical) complex; this type of near-IR absorption band has not been observed in any other metalloporphyrin π-cation radical complexes.

The π-cation radical [Fe(oxoOEC$^{\bullet}$)(Cl)]$SbCl_6$ shows a π-cation radical IR marker band at 1546 cm^{-1}. This band is similar to the π-cation radical IR marker bands found in octaethylporphyrinate and β-alkyl-substituted porphyrinate π-cation radical derivatives ($\sim$1550 cm^{-1}); *meso*-tetraaryl-substituted porphyrin π-cation radicals exhibit diagnostic π-cation radical IR marker bands at $\sim$1280 cm^{-1}.[44,45] It is also similar to the 1560 cm^{-1} marker band found in the π-cation radical [Cu(oxoOEC$^{\bullet}$)]-$SbCl_6$.[27] Upon oxidation of [Fe(oxoOEC)(Cl)] to [Fe(oxoOEC$^{\bullet}$)-(Cl)]$SbCl_6$, the carbonyl band in the infrared shifts from 1710 to 1730 cm^{-1}. This large oxidation-induced shift of the carbonyl band indicates that the oxidation of [Fe(oxoOEC)(Cl)] accompanies a significant change of the electronic structure of the macrocycle; a +20 cm^{-1} oxidation-induced shift of this band was also noted in the π-cation radical [Cu(oxoOEC$^{\bullet}$)]$SbCl_6$. The increase in energy of these carbonyl bands upon oxidation is consistent with the removal of electron density from the porphyrin ring, forming π-cation radicals.

The quadruple splittings and the isomer shift values for [Fe-

(oxoOEC)(Cl)] and [Fe(oxoOEC•)(Cl)]$SbCl_6$ are typical of five-coordinate high-spin ferric porphyrins (see Table 5).[51−53] The small Mössbauer quadrupole splitting constants for [Fe(oxoOEC)(Cl)] and [Fe(oxoOEC•)(Cl)]$SbCl_6$ clearly indicate that both iron centers are high spin. The isomer shift values are consistent with the assignment of a +3 oxidation state which further confirms the π-cation radical assignment of [Fe(oxoOEC•)(Cl)]-$SbCl_6$.

Structural Properties. The crystal structures of [Fe(oxoOEC)(Cl)] and [Fe(oxoOEC•)(Cl)]$SbCl_6$ have been determined. There are both structural and magnetic property differences that occur upon oxidation which are detailed herein.

Two types of M−N distances are observed in β-oxochlorin species: "short" M−N distances to the three pyrroles and a "longer" M−N distance to the pyrrolinone ring. In [Fe(oxoOEC)(Cl)], the "short" distances range from 2.058(4) to 2.066(4) Å, and the "long" distance is 2.125(5) Å. This bond distance difference is also found in all other crystallographically characterized metallo-β-oxochlorin, metallo-β-dioxoisobacteriochlorin, and metallo-β-trioxohexahydroporphyrin complexes including [Ni(oxoOEC)],[54,55] [Ni(dioxoOEiBC)],[55] [Ni(trioxoOEHP)],[55] [Cu(dioxoOEiBC)],[56] [Fe(dioxoOEiBC)(Cl)],[33] [Cu(oxoOEC)],[27] and [Cu(oxoOEC•)]$SbCl_6$.[27] Interestingly, after oxidation to [Fe(oxoOEC•)(Cl)]$SbCl_6$, the "long" Fe−N distance to the pyrrolinone ring decreases from 2.125(5) to 2.106(6) Å, while the average "short" Fe−N distance to the pyrrole rings does not change nearly as much (2.061(3) to 2.052(7) Å). This increased effect of oxidation on the metal−nitrogen bond of the pyrrolinone ring was seen even more dramatically in the oxidation of [Cu(oxoOEC)] to [Cu(oxoOEC•)]$SbCl_6$; the "long" Cu−N distance to the pyrrolinone ring decreased upon oxidation from 2.057(5) to 2.022(3) Å, while the average "short" Cu−N distance to the pyrrole rings stayed essentially the same (1.993(10) and 1.987(5) Å). The effects of oxidation on the "short" and "long" bond distances of the iron system studied here are not as large as in the copper system, and small differences in macrocyclic conformation may account for slight changes in Fe−N bond lengths (described below). However, it is apparent that the Fe−N pyrrolinone ring bond is affected more than the Fe−N pyrrole ring bonds upon oxidation of the macrocycle.

Various conformations have been found in metallo-β-oxoporphyrin systems. For example, [Cu(dioxoOEiBC)][56] is planar, [Cu(oxoOEC)] (general position) and [Cu(oxoOEC•)]-$SbCl_6$[27] are saddled, [Ni(trioxoOEHP)][55] is ruffled, and [Fe(dioxoOEiBC)(Cl)][33] has a domed conformation. The macrocycles of [Fe(oxoOEC)(Cl)] and [Fe(oxoOEC•)(Cl)]$SbCl_6$ are both saddled, and [Fe(oxoOEC•)(Cl)]$SbCl_6$ is slightly ruffled as well. It has been noted in some severely saddled π-cation radical systems that the magnitude of the saddle distortion increases upon oxidation.[24,25] For example, neutral [Cu(OETPP)][24] adopts a saddled conformation in which the β carbons are displaced by ±1.1−1.2 Å from the 24-atom mean plane. After oxidation, the saddling of the $[Cu(OETPP^{\bullet})]^+$ π-cation radical increases with the β-carbon displacements now at ± 1.36 Å.[24,25] In contrast to these observations and in accord with the results of the oxidation of [Cu(oxoOEC)] to the π-cation radical, [Cu(oxoOEC•)]$SbCl_6$, the magnitude of the saddle distortion decreases upon oxidation to [Fe(oxoOEC•)(Cl)]$SbCl_6$. The neutral [Fe(oxoOEC)(Cl)] complex has a saddled conformation with the β-carbon displacements ranging from ±0.10−0.22 Å and an absolute value average of 0.17(4) Å. After oxidation to the π-cation radical, [Fe(oxoOEC•)(Cl)]$SbCl_6$, the saddled distortion has β-carbon displacements of ±0.00−0.18 Å and an absolute average of 0.09(6) Å. The small differences in the average Fe−N bond lengths between [Fe(oxoOEC)(Cl)] ($Fe-N_{pyrrole}$ = 2.061(5), $Fe-N_{pyrrolinone}$ = 2.125(5)) and [Fe(oxoOEC•)(Cl)]$SbCl_6$ ($Fe-N_{pyrrole}$ = 2.052(7), $Fe-N_{pyrrolinone}$ = 2.106(6)) are, in part, the result of this decrease in saddling upon oxidation; it is expected that the macrocycle with the larger degree of saddling ([Fe(oxoOEC)(Cl)]) could have slightly longer Fe−N bond lengths.

The iron atoms in [Fe(oxoOEC)(Cl)] and [Fe(oxoOEC•)(Cl)]-$SbCl_6$ are displaced 0.46 and 0.49 Å out of the plane of the macrocycle (toward chloride), respectively. The magnitudes of these out-of-plane displacements are similar to the 0.47 Å displacement of the iron atom in [Fe(dioxoOEiBC)(Cl)] and typical of high-spin, pentacoordinate iron(III) porphyrins.[57,58] The axial Fe−Cl distances in [Fe(oxoOEC)(Cl)] and [Fe(oxoOEC•)(Cl)]$SbCl_6$ are 2.217(2) and 2.196(2) Å, respectively. These bond distances are comparable to those Fe−Cl distances found in five-coordinate, high-spin derivatives including chlorohemin[59] (2.218(6) Å) and [Fe(TPP)(Cl)][60] (2.211(1) Å). The chloride ligand "leans" toward the pyrrolinone ring in [Fe(oxoOEC)(Cl)]; the Cl−Fe−N angles to the pyrrole rings are 102.94(3), 105.86(13), and 104.85(13)°, while the Cl−Fe−N angle to the pyrrolinone ring is 96.40(13)°. The coordination of the chloride ligand is also irregular in the [Fe(dioxoOEiBC)(Cl)] complex; Cl−Fe−N bond angles range from 97.2(2) to 107.2(2)°, and the chloride points toward a pyrrolinone ring. The π-cation radical [Fe(oxoOEC•)(Cl)]$SbCl_6$ has a more regular coordination environment of the chloride ligand; Cl−Fe−N bond angles range from 100.1(2) to 105.4(2)°.

The pyrrolinone rings of [Fe(oxoOEC)(Cl)] and [Fe(oxoOEC•)(Cl)]$SbCl_6$ have lengthened $C_\beta-C_\beta$ bonds and widened $C_\beta-N-C_\beta$ angles as expected for such a saturated ring. The $C_\alpha-C_\beta$ bond containing the oxo substituent is shorter than the $C_\alpha-C_\beta$ bond containing the *gem*-diethyl group ($C_\alpha-C_{\beta(oxo)}$ 1.479(8) Å vs $C_\alpha-C_{\beta(gem-diethyl)}$ 1.514(8) Å for [Fe(oxoOEC)(Cl)] and $C_\alpha-C_{\beta(oxo)}$ 1.474(9) Å vs $C_\alpha-C_{\beta(gem-diethyl)}$ 1.487(10) Å for [Fe(oxoOEC•)(Cl)]$SbCl_6$); this suggests that the keto group is conjugated with the π system of the macrocycle.

A striking feature of the structure of [Fe(oxoOEC)(Cl)] is that all ethyl groups, except one *gem*-diethyl group, are on one side of the molecule (Figure 4a) and on the opposite side of the porphyrin from the single axial ligand. This type of structural feature is indicative[57] of minimal inter-ring $\pi-\pi$ interactions. Figure 4b shows a top-down view of an inversion-related pair of rings; for this pair the two iron centers are separated by 7.77 Å with a mean plane separation of 3.39 Å and a lateral shift of 7.39 Å.

The inter-ring geometry between the closest pair in [Fe(oxoOEC•)(Cl)]$SbCl_6$ is shown in Figure 5. The geometric parameters are quite different than those of the neutral precursor.

(51) Simonneaux, G.; Scholz, W. F.; Reed, C. A.; Lang, G. *Biochim. Biophys. Acta* **1982**, *716*, 1.
(52) Mashiko, T.; Kastner, M. E.; Spartalian, K.; Scheidt, W. R.; Reed, C. A. *J. Am. Chem. Soc.* **1978**, *100*, 6354.
(53) Sams, J. R.; Tsin, T. B. In *The Porphyrins*; Dolphin, D., Ed.; Academic Press: New York, 1978; Vol 4, pp 425−478.
(54) Stolzenberg, A. M.; Glazer, P. A.; Foxman, B. M. *Inorg. Chem.* **1986**, *25*, 983.
(55) Connick, P. A.; Haller, K. J.; Macor, K. A. *Inorg. Chem.* **1993**, *32*, 3256.
(56) Chang, C. K.; Barkigia, K. M.; Hanson, L. K.; Fajer, J. *J. Am. Chem. Soc.* **1986**, *108*, 1352.
(57) Scheidt, W. R.; Lee, Y. J. *Struct. Bonding (Berlin)* **1987**, *64*, 1.
(58) Scheidt, W. R.; Reed, C. A. *Chem. Rev.* **1981**, *81*, 543.
(59) Koenig, D. F. *Acta Crystallogr.* **1965**, *18*, 663.
(60) Scheidt, W. R.; Finnegan, M. G. *Acta Crystallogr., Sect. C* **1989**, *45*, 1214.

As shown in Table 4, the Fe···Fe distance, the lateral shift, and the mean plane separation all *increase* upon oxidation of [Fe(oxoOEC)(Cl)] to the π-cation radical; this is the inverse of what is usually observed on oxidation. In addition, there are large differences in the overlap orientation of the macrocycles of [Fe(oxoOEC)(Cl)] and [Fe(oxoOEC$^{\bullet}$)(Cl)]$SbCl_6$ (see top-down views, Figures 4b and 5b). Specifically, [Fe(oxoOEC)(Cl)] has no direct overlap; the dimeric unit has an "edge-to-edge" orientation. The top-down view of the [Fe(oxoOEC$^{\bullet}$)(Cl)]$SbCl_6$ dimer (Figure 5b) shows that the two porphyrin rings overlap at $C_\beta-C_\beta$. The two rings are related by a translation, and the two unique inter-ring atomic contacts are $C_{b1}\cdots C_{b6'} = 4.754$ Å and $C_{b2}\cdots C_{b5'} = 4.783$ Å; the closest inter-ring contact is $C_{b1}\cdots C_{62'} = 3.817$ Å.

The porphyrin−porphyrin ring overlap in this [Fe(oxoOEC$^{\bullet}$)(Cl)]$SbCl_6$ π-cation radical system is distinctly different from that of the four- and five-coordinate metallooctaethylporphyrinate (OEP) π-cation radical dimers.[20−22] The OEP π-cation radicals typically form tight cofacial dimers with small lateral shifts. Although such complete overlap of the two rings in [Fe(oxoOEC$^{\bullet}$)(Cl)]$SbCl_6$ is prevented by the *gem*-diethyl group, a larger degree of ring−ring overlap is possible. For example, [Cu(oxoOEC$^{\bullet}$)]$SbCl_6$[27] has a saw-tooth edge-over-edge interaction similar to that of the six-coordinate vanadyl octaethylporphyrinate π-cation radical, [$VO(OH_2)$(OEP$^{\bullet}$)]$SbCl_6$,[50] with unique inter-ring contacts of $C_{a6}\cdots C_{a7'} = 3.351$ Å and $C_{b5}\cdots C_{b8'} = 3.498$ Å. There is no evidence for an alternating long and short bond distance pattern[20−22,24,61] in this [Fe(oxoOEC$^{\bullet}$)(Cl)]$SbCl_6$ system.

Magnetic Properties. The magnetic susceptibility of [Fe(oxoOEC)(Cl)] and [Fe(oxoOEC$^{\bullet}$)(Cl)]$SbCl_6$ have been measured between 6 and 300 K. As described in the Results, the magnetic susceptibility of [Fe(oxoOEC)(Cl)] is typical of high-spin iron(III) porphyrinates. The Hamiltonian used in describing this $S = {}^5/_2$ system requires a zero-field splitting parameter of $D = 6$ cm^{-1} and an Fe···Fe interaction of $2J_{Fe-Fe} = -0.28$ cm^{-1}:

$$H = D[(S_z^2 - {}^1/_3S(S+1)) + (S_z'^2 - {}^1/_3S'(S'+1))] + g\beta\vec{H}(\vec{S}+\vec{S}') - 2J_{Fe-Fe}(\vec{S}\vec{S}')$$

Here D is the zero-field splitting parameter and S and S' are the two Fe spins.

The magnetic properties of [Fe(oxoOEC$^{\bullet}$)(Cl)]$SbCl_6$ are more complex. Given the minimal intermolecular overlap, our initial attempts to fit the magnetic susceptibility data assumed a simple monomeric model that involved intramolecular iron−radical coupling only (no intermolecular coupling). This model was unable to match the experimental data, especially in the low-temperature region. We thus used a model that also includes intermolecular contribution components. The magnetic exchange interactions involved in a laterally shifted dimeric [Fe(oxoOEC$^{\bullet}$)(Cl)]$SbCl_6$ complex can include both intramolecular iron−radical interactions and intermolecular interactions (radical−radical interactions and Fe···Fe interactions).

The temperature dependence of the experimental magnetic susceptibility for [Fe(oxoOEC$^{\bullet}$)(Cl)]$SbCl_6$ (Figure 6b) can be fit with a model that includes four terms in the total Hamiltonian: a zero-field splitting parameter, intramolecular magnetic coupling between the iron spin and the π-cation radical spin ($2J_{Fe-r}$), intermolecular coupling of the two iron spins ($2J_{Fe-Fe}$), and intermolecular coupling of the two radical spins ($2J_{r-r}$). The Hamiltonian of such a system is

$$H = D[(S_z^2 - {}^1/_3S(S+1)) + (S_z'^2 - {}^1/_3S'(S'+1))] + g\beta\vec{H}(\vec{S}+\vec{S}'+\vec{s}+\vec{s}') - 2J_{Fe-r}(\vec{S}\vec{s}+\vec{S}'\vec{s}') - 2J_{Fe-Fe}(\vec{S}\vec{S}') - 2J_{r-r}(\vec{s}\vec{s}')$$

where D is the zero-field splitting parameter, S and S' are the two Fe spins, and s and s' are the radical spins. It must be noted that D, $2J_{Fe-Fe}$, and $2J_{r-r}$ are strongly correlated in their effects on calculated susceptibilities. Because of the strong correlations among these three variables, we were not able to obtain a unique set of parameters to describe the experimental data. Thus, we have applied constraints on D and $2J_{Fe-Fe}$ using data from the best fit found for the neutral species [Fe(oxoOEC)(Cl)] (Figure 6a). We used the same zero-field splitting parameter ($D = 6$ cm^{-1}) as that determined for the neutral species. For $2J_{Fe-Fe}$, we used a value less than that of the best value (-0.28 cm^{-1}) for the neutral complex since the Fe···Fe separation in the radical is larger. A value of $2J_{Fe-Fe} = -0.14$ cm^{-1} was assigned, which leads to a value of -13 cm^{-1} for $2J_{r-r}$. The value of $2J_{r-r}$ is little affected by changes in $2J_{Fe-Fe}$ over the range of 0.0 to -0.28 cm^{-1}. A comparison of the fit of experimental and calculated susceptibilities, using these parameters, is shown in Figure 6b.

It is to be emphasized that an antiferromagnetic interaction between the two radical spins is required by the detailed temperature dependence of the magnetic susceptibility. This might be regarded as surprising given the large separation between the two rings, i.e, the large laterally shifted dimeric unit of [Fe(oxoOEC$^{\bullet}$)(Cl)]$SbCl_6$ (Figure 5) and the large inter-ring atom−atom separations. Two related π-cation derivatives, the six-coordinate vanadyl octaethylporphyrinate π-cation radical system, [$VO(OH_2)$(OEP$^{\bullet}$)]$SbCl_6$,[50] and the copper oxochlorin π-cation radical complex, [Cu(oxoOEC$^{\bullet}$)]$SbCl_6$,[27] also have rather large laterally shifted ring pairs and a large antiferromagnetic inter-ring interaction (coincidentally, $2J_{r-r} = -139$ cm^{-1} for both). The crucial difference between these latter two derivatives and the iron species appears to be the inter-ring interatomic distances: in the copper derivative there are nine such atom−atom contacts between 3.35 and 3.57 Å, and in the vanadyl derivative there are six such atom−atom contacts between 3.56 and 3.67 Å. In contrast, there are only two inter-ring contacts in the iron derivatives, which are much larger at 4.75 and 4.78 Å. The important conclusion is that even at these large distances there remains a nonzero radical−radical coupling path in [Fe(oxoOEC$^{\bullet}$)(Cl)]$SbCl_6$; indeed one that must be included in the overall coupling description to accurately describe the magnetochemistry of this unique compound. There may also be issues of precise inter-ring orientations that are important in defining the magnitude of the inter-ring radical coupling, but we do not have sufficient data at this time to comment on this issue.

Summary. We have reported the characterization of the metallooxooctaethylchlorin compound, [Fe(oxoOEC)(Cl)], and the one-electron oxidation product (the π-cation radical) [Fe(oxoOEC$^{\bullet}$)(Cl)]$SbCl_6$. The formation of tight cofacial dimeric units, which are characteristic of metallooctaethylporphyrin π-cation radicals, is inhibited by the modification at the periphery of the porphyrin ring. Although the dimeric unit has a large lateral shift, mean plane separation, and center···center distance, there is a weak intermolecular antiferromagnetic

(61) Brancato-Buentello, K. E.; Scheidt, W. R. *Angew. Chem., Int. Ed. Engl.* **1997**, *36*, 1456.
(62) Phillippi, M. A.; Goff, H. M. *J. Am. Chem. Soc.* **1982**, *104*, 6026.
(63) Maeda, Y.; Morita, Y. *Biochem. Biophys. Res. Commun.* **1967**, *29*, 680.
(64) Fitzsimmons, B. W.; Sams, J. R.; Tsin, T. B. *Chem. Phys. Lett.* **1976**, *38*, 588.

interaction between the radical spins in the dimeric unit. We have been able to obtain reasonable estimates of the various inter- and intramolecular coupling components by the complementary use of X-ray crystallography, temperature-dependent magnetic susceptibility measurements, and Mössbauer and UV/vis/near-IR spectroscopy.

Acknowledgment. We thank the National Institutes of Health for support of this research under Grant GM-38401 (W.R.S.) and for the purchase of X-ray instrumentation under Grant RR-06709. We also thank the National Science Foundation for the purchase of the SQUID equipment under Grant DMR-9703732.

Supporting Information Available: Figure S1, displaying the zero-field Mössbauer spectra of [Fe(oxoOEC)(Cl)] and [Fe(oxoOEC$^{\bullet}$)(Cl)]$SbCl_6$ at 4.2 K, Figure S2, displaying the plot of absorbance vs concentration of the near-IR absorption band in [Fe(oxoOEC$^{\bullet}$)(Cl)]$SbCl_6$, Tables S1−S12, giving complete crystallographic details, complete bond distances and angles, anisotropic temperature factors, and fixed hydrogen atom positions for both complexes, and CIF files. This material is available free of charge via the Internet at http://pubs.acs.org.

IC991052W